Two-phase flow in compressed copper foam with R134a for high heat flux thermal management: Effects of foam compression ratio and refrigerant operating conditions on thermohydraulic performance

*Deogratius Kisitu¹, Alfonso Ortega¹, Metodi Zlatinov², Denver Schaffarzick²

¹NSF – Center for Energy-Smart Electronic Systems (ES2), Villanova University, Villanova, PA, USA

²ERG Aerospace Corporation, Oakland, CA, USA

*dkisitu@villanova.edu

Abstract—Most previous research in metallic open-cell foams has focused on single-phase cooling with air or with water. This work examines the thermohydraulic performance of open-cell copper foam with R134-a refrigerant in two-phase flow boiling conditions at heat fluxes well above those examined in majority of previous studies. Detailed experimental results are presented for the thermal performance and pressure drop of copper foam media, in geometric configurations similar to that which may be utilized in a two-phase cold plate. Key to the present study is an investigation of the effects of compression of the foam on its thermohydraulic behavior and critical heat flux (CHF) during flow boiling. The test coupons consist of foam samples, each with a footprint of 25.4 mm x 25.4 mm and a height of 2.54 mm, which are soldered to a copper base plate. The foam samples include a baseline uncompressed sample, and two other samples with compression ratios (CR) of 2X and 4X, with porosities of 0.91, 0.82 and 0.62, respectively, and each with a pore size of 40 PPI. The test coupons are mounted in an engineered flow fixture that allows refrigerant flow to enter in an inlet manifold, then through the foam, before flowing to an exit manifold. Experimental tests were performed for heat fluxes from 1.4 to 175 W/cm², with mass fluxes ranging from 125 to 250 kg/m²s and inlet saturation temperatures of 30 to 40 °C, while varying the inlet subcooling from 0 to 20 °C. Results show that thermal resistance, optimum exit vapor quality, CHF, and pressure drop for flow boiling in compressed metal foams depend strongly on foam compression ratio, inlet subcooling and saturation temperature.

Keywords—Compressed foams, Porous media, Two-phase Cooling, Boiling, Subcooling, High heat flux, Electronics cooling

NOMENCLATURE

A	Footprint area, m^2
C_p	Specific heat Capacity, $J/kg \cdot K$
CHF	Critical Heat Flux, W/m^2
CPU	Central Processing Unit

CR	Compression ratio (X)
G	Effective mass flux, $kg/m^2 \cdot s$
$G\!PU$	Graphics Processing Unit
h	Specific enthalpy, J/kg
I	Current, A
k	Thermal conductivity, $W/m \cdot K$
L	Base plate length, <i>m</i>
i ·	Mass flow rate, kg/s
P	Pressure, Pa
PCM	Phase Change Material
PPI	Pores Per Inch
<i>PSU</i>	Power Supply Unit
Q	Power, W
q''	Heat flux, W/m^2
R''	Unit thermal resistance, $K \cdot m^2/W$
t	Thickness, m
T	Temperature, K
TIM	Thermal Interface Material
TTV	Thermal Test Vehicle
V	Voltage, V
W	Width, m
x	Vapor quality
X	Streamwise direction
Y	Vertical direction
Z	Spanwise direction
Greek Symbols	
ΔP	Pressure drop, Pa
ΔT	Temperature difference, K
\mathcal{E}	Porosity
Subscripts	
	A a4a1

Actual

Base

act base

Copper CuElectrical ele fm Foam L Liquid phase VVapor phase in Inlet Mean mean. Refrigerant ref Outlet/Exit out sat Saturation Subcooling sub Superheat sup Wall wall

I. INTRODUCTION

The era of modern, high-performance electronics, including microprocessors (CPU's and GPU's), power electronics, aerospace, defense, and others, is unprecedentedly skyrocketing the heat fluxes [1], [2]. Air cooling limits are being reached [3]. Ortega et al. [4] investigated limits for pumped liquid cooling using a modified effectiveness-NTU cold plate model. Given the fact that limits for both the conventional air and liquid cooling are being approached, more innovative, advanced thermal management solutions, mainly using two-phase cooling, are urgently needed. Traditionally, microchannels have been investigated and used in pumped two-phase cooling. Kandlikar et al. [5] reported major challenges hampering their microchannels practical application, among which included low CHF, flow instability, high pressure drop, clogging and others.

Apart from microchannel flow boiling, two-phase flow in other heat transfer enhancement structures, including open-cell metal foams, have been investigated for indirect two-phase cooling, although, these studies are few [6]. Kim et al. [7] investigated two-phase flow characteristics of three uncompressed copper foams, with 95% porosity and 10 PPI, 95% porosity and 20 PPI, and 92% porosity and 20 PPI. Heat fluxes from 6 to 27 W/cm² and mass fluxes from 20 to 72 kg/m²s were tested. Data revealed that the foam sample with high porosity and large pore size (95% porosity and 10 PPI) had the best thermal performance. It was revealed that foam porosity weakly influences the heat transfer coefficient at high heat fluxes by up to 23%, and larger pore size gave higher heat transfer enhancement for a fixed porosity.

Using FC-72, Pranoto and Leong [8] studied flow boiling in evaporators with graphite porous foams with porosities of 61% and 72%, and with bypass gaps of 6, 4, and 2 mm. Heat fluxes of 4 to 83.3 W/cm² and mass fluxes of 50, 100, and 150 kg/m²s were tested. Data revealed that graphite foams of 61% and 72% porosities enhanced the heat transfer coefficients by up to 2.5 and 1.9 times, in comparison to a bare surface. The highest local heat transfer coefficient of 16.5 kW/m²K was achieved with 61%-porosity foam at a mass flux of 150 kg/m²s and a 6 mm gap. Their high-speed visualization studies revealed that more bubble departure frequency was observed from the 61%-porosity foam, resulting from more active nucleation sites, which resulted to a higher thermal performance enhancement.

Madani et al. [9] studied two-phase flow inside a vertically oriented channel filled with 97%-porosity and 36 PPI uncompressed copper foam with n-pentane as a working fluid. Heat fluxes from 0 to 25 W/cm² and mass fluxes ranging from 10 to 100 kg/m²s were investigated. Comparing their results with the Gungore-Winterton correlation [10] revealed that the metallic foam insert increases the heat transfer coefficient up to 4-fold, at low quality.

In another study, the thermohydraulic performance of R134a and R1234ze(E) with single-phase and two-phase flow in a 5 PPI uncompressed copper foam was investigated by Mancin et al. [11]. Heat fluxes of 5 and 10 W/cm² and mass fluxes of ranging from 50 to 200 kg/m²s were tested at an inlet saturation temperature of 30 °C. Data revealed that R134a two-phase flow performs better than that of R1234ze. The study in [11] was later extended by Diani et al. [12], using in the same test setup and the thermal performance of R1234vf, R1234ze(E) and R134a were investigated during flow boiling. Their data reveal that the pressure drops increase linearly with both vapor quality and mass flux for all refrigerants, with R1234ze(E) having the greatest pressure drops, particularly at high mass flux. Results showed that heat transfer coefficients could be increased by more than 4 times, in comparison to the predictions by Gungor-Winterton correlation [10]. It was experimentally demonstrated that R134a has the best thermal performance, followed by R1234yf.

The above-cited studies show that two-phase flow investigations in metallic foams were mainly centered on uncompressed samples at low heat fluxes. In the current study, one aim is to explore the performance at heat fluxes that would arise in high performance applications such as in electronic devices. It was previously reported that compressing metallic foam in streamwise (X – direction) direction proportionally increases thermal conductivity as the compression ratio increases [6], [13]. It was also revealed that streamwise foam compression keeps the pores open to the approaching flow, thus reducing pressure drop, in comparison to compressing in other directions (Z and Y – directions) [6]. Kisitu et al. [6] originally investigated the use of compressed foams as alternatives to microchannels for pumped indirect two-phase cooling and promising results were reported. Two copper foam samples, one uncompressed (1X) and the second one compressed four times in the streamwise direction (4X) were studied, with porosities of 91% and 62% respectively, and each with a PPI of 40 and thickness of 0.25 cm and with heated footprint area of 2.54x2.54 cm². Heat fluxes from 7 to 174 W/cm² and mass fluxes ranging from 150 to 375 kg/m²s were tested at inlet saturation temperatures of 31 to 33 °C with inlet subcooling from 1 to 3 °C. Their data revealed that compressing copper foam by 4X enhanced thermal performance by more than 300%, attributed to smaller effective hydraulic diameter, higher surface area per unit volume, and higher bulk thermal conductivity. Results also showed that higher heat transfer coefficient can be obtained in compressed 4X foam, which maximizes at optimum exit vapor qualities of about 70 to 75%, beyond which it degrades. It was further found that no flow instabilities were observed in compressed 4X foam, even at high heat and mass fluxes tested, which is in contrast to flow boiling in microchannels.

The present work continues the recent study by Kisitu et al. [6] on compressed metallic foam two-phase flow. Using the same well-calibrated two-phase flow experimental rig, experimental investigations were conducted to understand the effects of foam compression ratio (CR) and refrigerant operating conditions, including inlet subcooling and inlet saturation temperature on the two-phase flow and heat transfer. The data will show that flow boiling performance in metallic foams is a strong function of foam compression, inlet subcooling, and saturation temperature.

II. EXPERIMENTAL TESTING

A. Experimental Setup and Schematic

Figure 1 shows the schematic of the two-phase flow loop which was designed to control and measure the test section inlet conditions, the same used in previous study [6]. The two-phase flow loop is divided into three sections, including the test section, the condenser section, and the flow conditioning section. The brazed plate heat exchanger condenser, located upstream of the test section, rejects heat, which is achieved by a NESLAB™ HX Series Recirculating Chiller that controls the condensation temperature. After condensation, the saturated liquid refrigerant is stored in the stainless-steel reservoir which is instrumented with a 1/8 in type-K thermocouple probe and a 0-300 psi OmegaTM PX209 pressure transducer. The reservoir attains saturation conditions and thus equilibrates to its saturation pressure at the reservoir temperature. The liquid refrigerant from the base of the reservoir is pumped by a Tuthill gear pump with a DART digital speed controller aiding in controlling the mass flow rate (pump motor RPM). The liquid leaving the pump is filtered and the flow is then metered by an EmersonTM Micro Motion® ELITE® Coriolis flowmeter. Lastly, the fluid temperature is precisely controlled by passing the flow through a copper coiled-tube heat exchanger immersed in a ThermoNESLAB isothermal bath, which allows precise control of the fluid temperature at the entry of the evaporator. The inlet temperature and pressure are measured using an inline 1/8 in type-K thermocouple probe and a 0-300 psi OmegaTM PX209 pressure transducer, respectively. The evaporator average base temperature is measured at the center of the base with a butt-welded type-K thermocouple embedded in a groove that is machined in the base. The pressure drop across the evaporator is measured using a 0-50 psid SetraTM DPT2301 differential pressure transducer. The temperature of the twophase mixture leaving the evaporator is measured by an inline 1/8 in type-K thermocouple probe.

B. Evaporator Test Section

The test section assembly, Fig. 2 (a), which is the same as used in [6], consists of stainless evaporator housing the foam sample. The "lid" is a transparent window to aid in flow visualization. Transparent tubes are connected to the inlet and exit of the evaporator to visually monitor the vapor qualities of the fluid entering and exiting the test section. The evaporator base is constructed so as to facilitate the flow to enter the inlet manifold from below and leave through the outlet manifold through flow

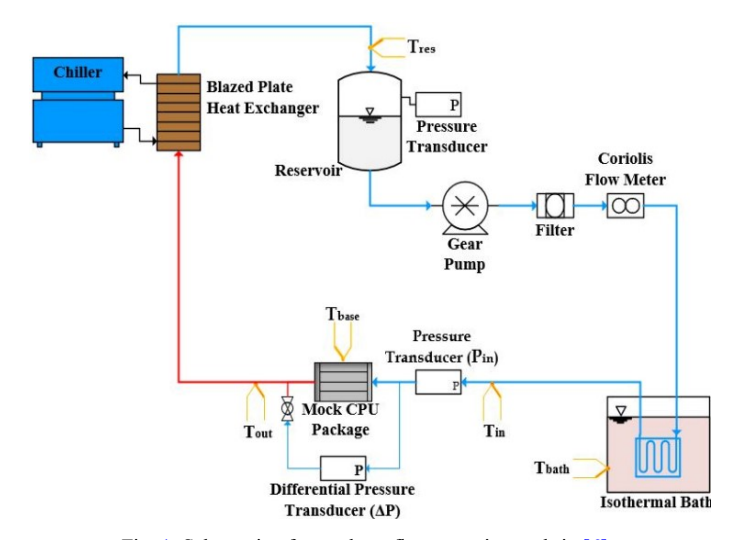


Fig. 1. Schematic of two-phase flow experimental rig [6]

ports that match the ports in the manifolds of the foam sample, as show in Fig. 2 (c). The foam sample is soldered to the base plate. Uniform heating is applied to the base plate by a heat concentrator bar with the same cross-sectional area (2.54 x 2.54 cm) as the footprint area of the foam sample mounted on it. Thus, there is very little heat spreading in the evaporator base. The evaporator assembly is mounted onto the top surface of the heater bar with a spring-loaded mechanism as shown in Fig. 2 (a). The spring loader allows a repeatable uniform loading pressure of about 30 psi to be applied to the base plate by the heat bar. To minimize thermal contact resistance between the evaporator base and concentrator bar, a phase change TIM (Honeywell PTM 7950) with thermal conductivity of about 8.5 W/m-K [14], was used between the base plate and the concentrator. The heat concentrator bar, Fig. 2 (b), was fabricated from copper with a bar of cross section area of 1 in. x 1 in., which transitions into a larger base in which four Tempco cartridge heaters are installed. The Tempco heaters were connected in parallel and supplied by a KEYSIGHT N8762A DC power supply unit (PSU). Equally spaced type-K thermocouples installed in the concentrator bar centerline allowed the measurement of the temperature gradient through the bar. Application of Fourier's Law was utilized to determine the heat flux applied to the evaporator base.

C. Test Foam Samples

ERG Aerospace Duocel® foam test samples [15] with compression ratios of 1X, 2X and 4X were soldered to a machined pocket in the copper base plate, with inlet and outlet flow ports entering the inlet and exit manifolds as seen in Fig. 2. The foam samples had a footprint of 2.54 x 2.54 cm and were 0.254 cm in thickness. The base thickness is 0.2 cm. Copper foam samples were soldered onto the bases in an inert environment using SAC 305 (96.5% Sn, 3% Ag, and 0.5% Cu) solder foil [6]. Fig. 3 illustrates the three investigated foam samples, including 1X (porosity of 91%), 2X (porosity of 82%) and 4X (porosity of 62%).

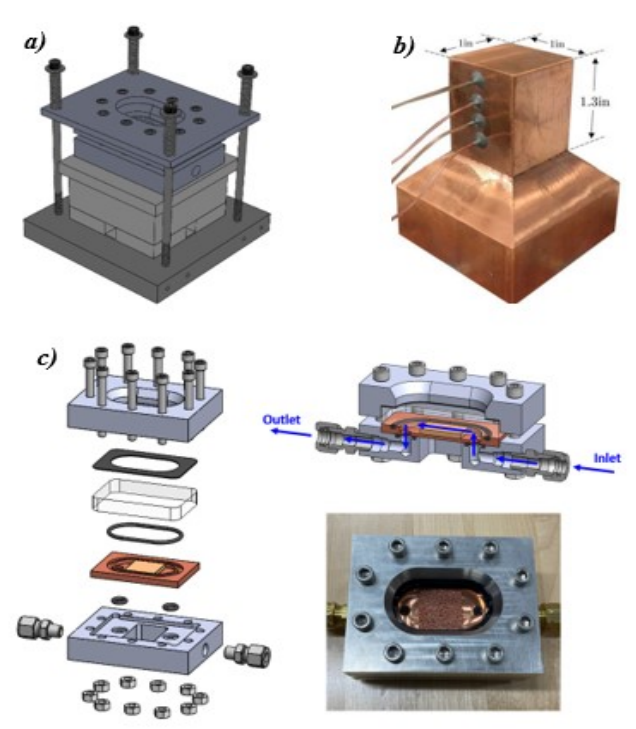


Fig. 2. (a) Test section assembly, (b) Concentrator (TTV), and (c) Test section assembly with exploded view and flow configuration [6]

TABLE 1. FOAM CHARACTERISTICS PROVIDED BY ERG AEROSPACE CORPORATION [15]

Foam Sample		1X	2X	4X
	Foam Length (L _{fm}) [mm]	25.4	25.4	25.4
nodi	Foam Width (W_{fm}) [mm]	25.4	25.4	25.4
Test Coupon	Foam Thickness (t_{fm}) [mm]	2.5	2.5	2.5
Tes	Base Area (A_{base}) $[cm^2]$	6.45	6.45	6.45
	Base Thickness [mm]	2.0	2.0	2.0
	PPI	40	40	40
	Nominal Compression Ratio (CR)	-	2	4
	Compress Direction	-	X	X
E	Initial Porosity	0.91	0.90	0.90
Foam	Final Porosity	0.91	0.82	0.62
	Effective Compression Ratio (CR)	1.00	1.96	3.85
	Surface Area per Unit Volume [in²/in³]	23	45	90
	Foam Material	C10100	C10100	C10100
al vity	k_{Cu} [W/m-K]	390	390	390
Thermal onductivi	$k_{fm,X} [\mathrm{W/m\text{-}K}]$	12.0	6.2	3.3
Thermal Conductivity	$k_{fm,Y}$ [W/m-K] (heat flux direction)	12.0	23.5	49.5
	$k_{fm,Z}$ [W/m-K]	12.0	23.5	49.5

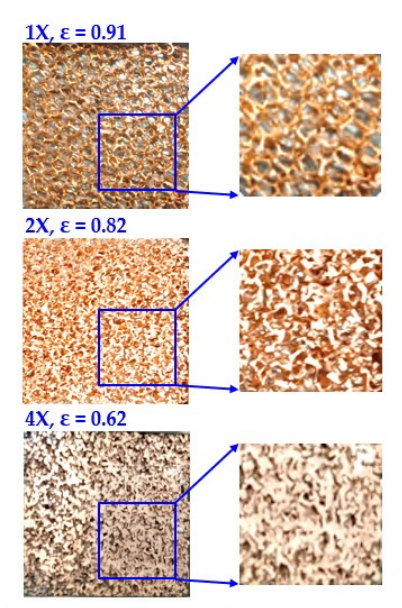


Fig. 3. 1 in x 1 in uncompressed (1X) and compressed (2X and 4X) test foam coupons manufactured by ERG Aerospace Corporation [15]

Detailed properties of the subject foam samples were provided by the manufacturer [15] and summarized in Table. 1.

D. Test procedure

Experimental tests were conducted using R134a as the refrigerant. The effect of foam compression ratio on thermal resistance, critical heat flux (CHF), and pressure drop were studied by separately testing three foam coupons (1X, 2X and 4X) under the same thermal and flow conditions. A constant inlet saturation temperature of 40 °C and inlet subcooling of 3 °C was considered for these comparison tests. To investigate the influence of inlet subcooling on performance, flow boiling tests with compressed 4X foam were conducted with an inlet saturation temperature of 30 °C maintained constant while varying the inlet fluid temperature from 30 to 10 °C, thus varying the inlet subcooling temperatures from 0 to 20 °C. A fixed mass flow rate of 6 g/s (150 kg/m²s) were used. Three heat flux were tested in this portion of the study, including 25, 50 and 100 W/cm². Lastly, to examine the effect of inlet saturation temperature on flow boiling in compressed foam (4X), two inlet saturation temperatures of 30 °C and 40 °C were distinctly studied, while maintaining other test conditions identical. CoolProp [16] was used to obtain the thermophysical properties of the working fluid (R134a) at all the considered fluid states.

E. Data Reduction

The electrical power, Q_{ele} supplied to the thermal test vehicle (TTV) or concentrator cartridge heaters was defined as below. The current and the voltage were digitally displayed by the calibrated Keysight power supply unit.

$$Q_{\rho l \rho} = I \cdot V \tag{1}$$

The actual heat flux applied to the base of the foam evaporator was precisely determined from Fourier's law of 1-D

steady-state conduction using the temperatures measured by equally spaced thermocouples installed in the heat concentrator column, as shown in Fig. 2 (b)

$$q'' = -k_{Cu} \frac{dT}{dx} \tag{2}$$

The actual electrical power input to the base of the foam evaporator was computed from the product of actual heat flux (from Eqn. 2) and the footprint area of the concentrator TTV top, which is the same as foam evaporator base area:

$$Q_{act} = q'' \cdot A_{base} \tag{3}$$

The electrical power losses were computed using Eqn.4. In this setup, the estimated average power loss was about 6%.

$$Q_{loss} = Q_{ele} - Q_{act} \tag{4}$$

The vapor quality of the two-phase mixture exiting the foam evaporator or test section was expressed as:

$$x_{out} = \frac{h_{out} - h_L}{h_V - h_I} \tag{5}$$

Where, the exit specific enthalpy of the foam evaporator, h_{out} can be obtained from an energy balance analysis assessed on the evaporator/test section:

$$h_{out} = h_{in} + \frac{Q_{act}}{i} \tag{6}$$

The inlet specific enthalpy was obtained as a function of inlet fluid pressure and temperature.

$$h_{in} = h(P_{in}, T_{in}) \tag{7}$$

The saturated liquid/fluid and vapor/gas specific enthalpies, h_L and h_V , respectively, were obtained as a function of the exit saturation pressure of the foam evaporator.

$$h_L = h(P_{sat.out}) \tag{8}$$

$$h_V = h(P_{sat out}) \tag{9}$$

The foam evaporator unit thermal resistance, R'' was intentionally defined with a reference temperature as the inlet fluid temperature, T_{in} to account for the effects of subcooling, as also defined in [6].

$$R'' = \frac{\left(T_{base} - T_{in}\right)}{q''} \tag{10}$$

The inlet subcooling temperature was obtained as a function inlet saturation temperature and the inlet temperature.

$$\Delta T_{sub} = T_{sat.in} - T_{in} \tag{11}$$

The wall superheat was defined as a function of wall temperature and mean saturation temperature.

$$\Delta T_{sup} = T_{wall} - T_{sat,mean} \tag{12}$$

The mean saturation temperature was computed as arithmetic mean of the inlet and outlet saturation temperatures [6], [12]:

$$T_{sat,mean} = \frac{\left(T_{sat,in} + T_{sat,out}\right)}{2} \tag{13}$$

The mass flux through the metallic foam evaporator was expressed as a function of porosity, as was defined in [6].

$$G = \frac{i}{\varepsilon_{fin}} \cdot W \cdot t \tag{14}$$

F. Uncertainty analysis

All of the measurement instruments were first calibrated before taking experimental data to minimize uncertainty. Table. 2 summarizes the systematic uncertainty of several measured variables derived from the instruments used.

TABLE 2. UNCERTAINTY OF MEASURED VARIABLES

Measured variable	Uncertainty
Temperature (Type-K Thermocouples)	±0.15 ℃
Pressure drop (0-50 psid Setra TM DPT2301	$\pm 0.25\%$ of full scale
differential pressure transducer)	
Saturation pressure (0-300 psi Omega TM	$\pm 0.25\%$ of full scale
PX209 pressure transducer)	
Mass flow rate (Emerson TM Micro Motion®	$\pm 0.10\%$ of the reading
ELITE® Coriolis flowmeter)	
Power (Keysight N8762A DC PSU)	\pm 0.025% (Voltage) and
	±0.1% (Current)

The uncertainties propagated to variables (heat flux and thermal resistance) computed from experimental measurements were calculated from a proposed method by Moffat [17]. Table 3 shows the uncertainties derived from Eqns. 15 and 16.

$$\delta q'' = \sqrt{\frac{\left(\frac{\partial q''}{\partial k_{Cu}} * \delta k_{Cu}\right)^2 + \left(\frac{\partial q''}{\partial T_1} * \delta T_1\right)^2 + \left(\frac{\partial q''}{\partial T_2} * \delta T_2\right)^2 + \left(\frac{\partial q''}{\partial l_{1-2}} * \delta l_{1-2}\right)^2}$$

$$(15)$$

$$\delta R^{"} = \sqrt{\left(\frac{\partial R^{"}}{\partial T_{base}} * \delta T_{base}\right)^{2} + \left(\frac{\partial R^{"}}{\partial T_{in}} * \delta T_{in}\right)^{2} + \left(\frac{\partial R^{"}}{\partial q^{"}} * \delta q^{"}\right)^{2}}$$
(16)

TABLE 3: UNCERTAINTY OF CALCULATED VARIABLES

Calculated variable	Uncertainty	
Heat flux, q"	±3.61%	
Thermal resistance, R"	±5.02%	

RESULTS AND DISCUSSION

A. Effect of Compression Ratio (CR) on Performance

The influence of foam compression ratio, including 1X, 2X and 4X, on both the thermal performance (thermal resistance and CHF) and pressure drop was investigated at a fixed inlet saturation temperature of 40 °C and an inlet subcooling of 3 °C. From Fig. 4, data show that the thermal resistance is strongly dependent on compression ratio (X or CR), defined as initial volume divided by final volume. Increasing the compression ratio decreases the thermal resistance. For instance, at a high heat flux of about 100W/cm², results clearly reveal that 4X and 2X reduces thermal resistance by 671% and 285%, respectively, compared to the uncompressed (1X) sample. Similar observations were reported in the previous study by

Kisitu, et al. [6]. This is because increasing the compression ratio proportionally increases surface area per unit volume and bulk thermal conductivity (in upward heat flux direction) of foam and decreases the hydraulic pore diameters, which all enhance thermal performance for two-phase flow boiling.

Data, in Fig.4, also reveal that at low heat fluxes, thermal resistance decrease rapidly with increase in heat flux for all compression ratios indicating nucleate boiling dominance. For only compressed foams (2X and 4X), from medium to high heat fluxes, results show that thermal resistance become almost insensitive to increase in heat flux at a fixed mass flux, which most likely indicates that convective boiling dominates.

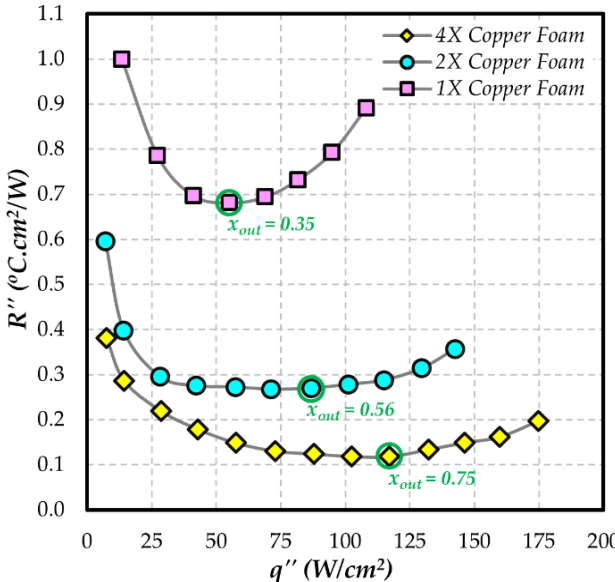


Fig. 4. Effect of foam compression ratio (CR) on unit thermal resistance and optimum exit quality (x_{out}) at \dot{m}_{ref} of 6 g/s, $T_{sat, in}$ of 40 °C and ΔT_{sub} of 3 °C

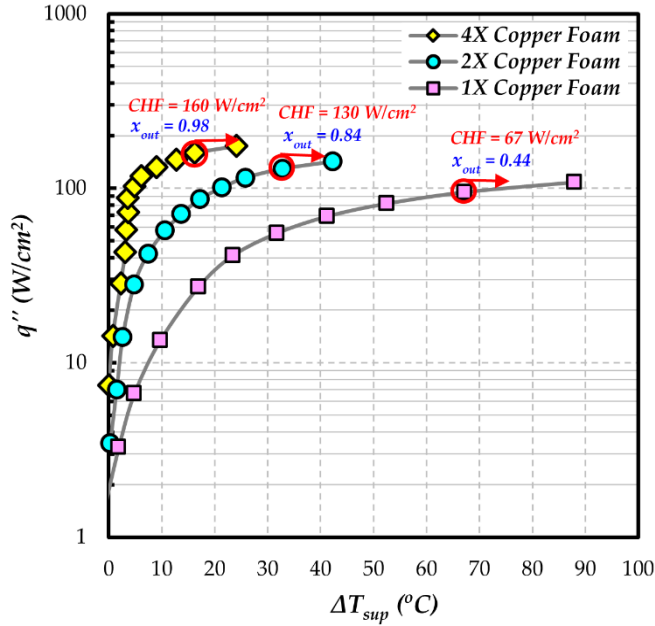


Fig. 5. Effect of foam compression ratio on the critical heat flux (CHF) and critical exit quality (x_{out}) at \dot{m}_{ref} of 6 g/s, $T_{sat, in}$ of 40 °C and ΔT_{sub} of 3 °C

In addition, for each foam sample, data show that thermal resistance minimizes at a unique heat flux or optimum exit vapor quality, beyond which it increases. This is attributed to the accumulation of vapor in the two-phase mixture at increased heat flux or vapor qualities, which deteriorates the thermal conductivity of fluid mixture and thus degrade the heat transfer coefficient when the optimum exit vapor quality is exceeded, as shown in Fig. 4. It is observed that compressing the foam enhances that optimum exit quality at which maximum thermal performance (lowest resistance) is obtained. An optimum exit quality as high as 75% is attained by 4X foam and similar results were reported by Kisitu et al. [6]. Present data reveal that 4X and 2X significantly increased the optimum exit vapor quality by 214% and 160%, respectively, compared to the uncompressed (1X) foam.

Figure. 5 shows the boiling curves of two-phase flow in 1X, 2X and 4X foams and the same were based on to investigate the effect of compression ratio on critical heat flux (CHF), the same CHF criteria previously used by Ong and Thome [18]. It is shown that at fixed conditions, CHF in metal foams is strongly dependent on compression ratio (CR). CHF in foam increases monotonically with increase in compression ratio. This is most likely attributed to the possibility that increase in compression ratio increases wetted/replenished area and active nucleation site density, which all together increase the heat transfer coefficient as well as delaying the occurrence of burn out or dry out crisis, thus significantly increasing CHF. With the present test conditions, data show that 4X and 2X compressed foams enhanced CHF by almost 240% and 194%, respectively, compared to the baseline or uncompressed (1X) foam sample. Another interesting observation is that the critical exit vapor quality (the exit quality at which CHF occurs) for two-phase flow in foam increases with increase in compression ratio, as

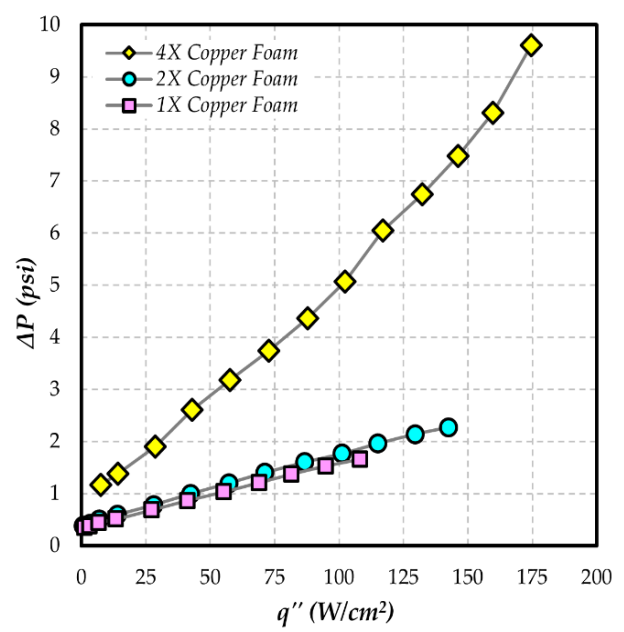


Fig. 6. Effect of foam compression ratio (CR) on pressure drop at \dot{m}_{ref} of 6 g/s, $T_{\rm sat, in}$ of 40 °C and $\Delta T_{\rm sub}$ of 3 °C

illustrated in Fig. 5, which is significantly important. Data, in Fig. 5, show that 4X and 2X enhanced the critical exit quality 2.23 and 1.17 times, respectively, compared to the uncompressed (1X) foam counterpart.

From the hydraulic performance standpoint, results show, in Fig. 6, that pressure drop increases with increase in compression, as also reported in [6]. This is attributed to decrease in the hydraulic diameter as the compression ratio increases, thus resulting in more flow resistance, for a given mass flow rate. It should be noted that pressure drop for 2X is slightly higher than 1X and further investigation is ongoing to understand what this is attributed to.

B. Effect of Refrigerant Operating Conditions on Performance

1) Inlet Saturation Temperature

effect of inlet saturation temperature thermohydraulic performance was studied on two-phase flow in 4X compressed copper foam. Tests were conducted at a fixed inlet subcooling of 3 °C and two saturation temperatures of 30 °C and 40 °C were investigated. Data reveal that the thermal resistance in 4X foam is a strong function of inlet saturation temperature. For the abovementioned fixed conditions, thermal resistance decreases with increase in inlet saturation temperature, as shown in Fig. 7. However, despite the lower thermal resistance attained at higher inlet saturation temperature, it should be noted that the evaporator base temperatures are lower for lower inlet saturation temperatures, for fixed conditions. As such, if the thermal design goal is to have lower base temperature, lower inlet saturation temperatures are recommended, though there is a penalty on higher chiller power required, compared to the higher inlet saturation temperature case.

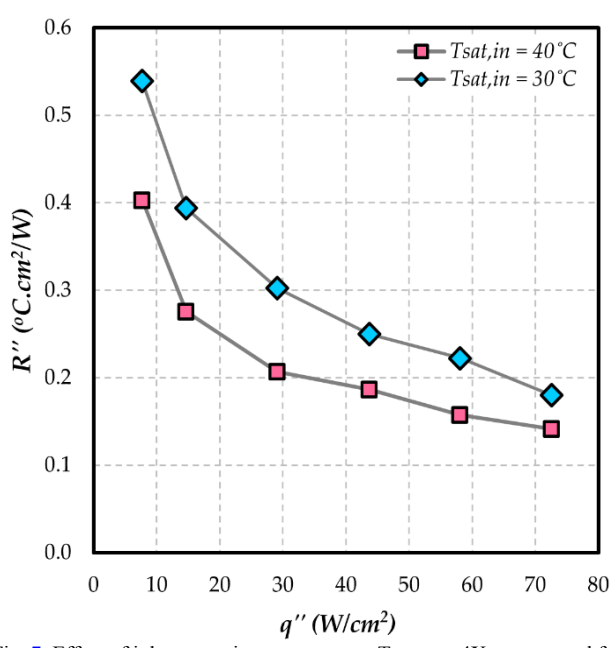


Fig. 7. Effect of inlet saturation temperature, $T_{sat, in}$, on 4X compressed foam thermal resistance at G of 200 kg/m²s and ΔT_{sub} of 3 °C

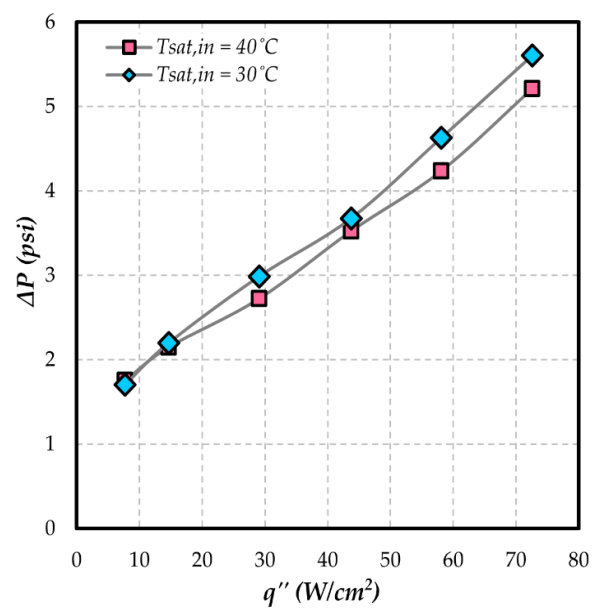


Fig. 8. Effect of inlet saturation temperature, $T_{sat, in}$ on 4X compressed foam pressure drop at G of 200 kg/m²s and ΔT_{sub} of 3 °C

Fig. 8 shows that pressure drop at inlet saturation temperature of 30 °C is slightly higher than that at 40 °C, for given fixed conditions. Thus, pressure drop in 4X foam has a weak dependence on inlet saturation temperature.

2) Influence of Inlet Subcooling Temperature

Results show that thermal resistance is a strong function of inlet subcooling, as shown in Fig. 9. Thermal resistance increase with increase in inlet subcooling due to burgeoning portion of foam in single phase regime with low heat transfer coefficients. Fig. 10. shows that increasing subcooling proportionally decrease the exit quality and thermal resistance

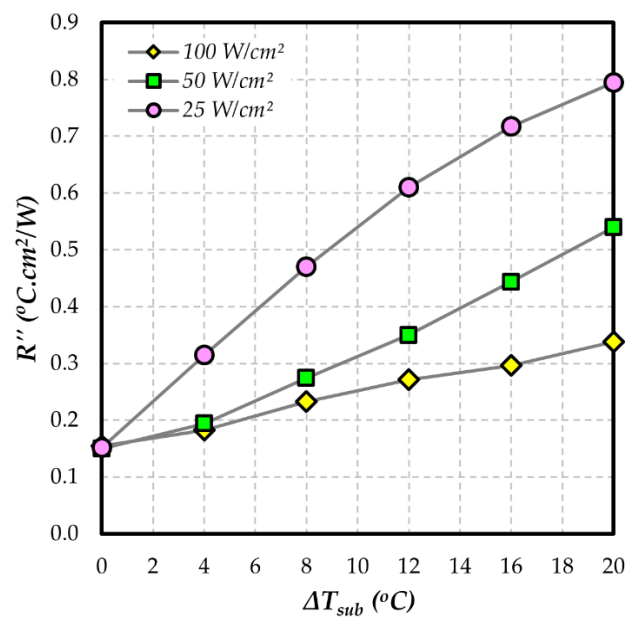


Fig. 9. Effect of inlet subcooling on 4X compressed foam thermal resistance at G of 150 kg/m²s and $T_{sat, in}$ of 30 °C

decrease with increase in vapor quality. This indicates dominance of nucleate boiling.

Most important, the current data (Fig. 10) reveal that with 0% exit quality (single-phase), thermal resistance will be similar regardless of the heat flux, which is due to single-phase cooling dominance. From Fig. 9 and 10, as expected, the data confirm that the minimum thermal resistance is always attained when saturated liquid (0 °C inlet subcooling) is used at the inlet.

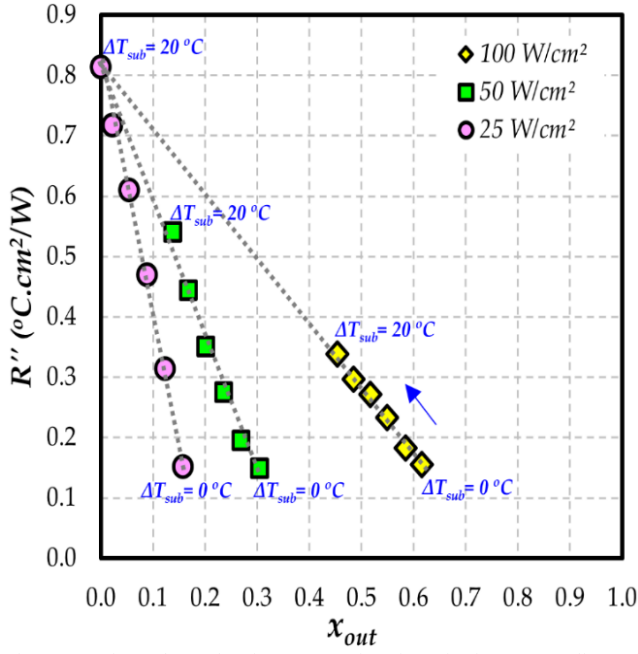


Fig. 10. 4X foam thermal resistance as a function of exit vapor quality and inlet subcooling at *G* of 150 kg/m²s and T_{sat in} of 30 °C

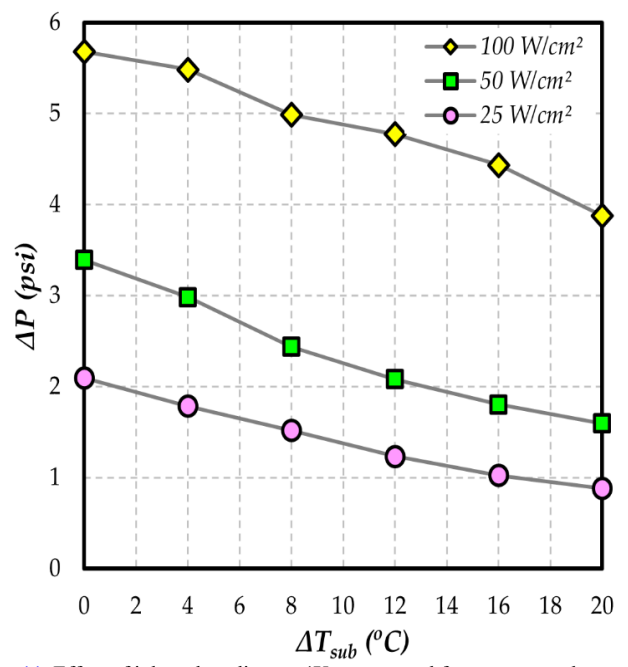


Fig. 11. Effect of inlet subcooling on 4X compressed foam pressure drop at G of 150 kg/m²s and $T_{\text{sat. in}}$ of 30 °C

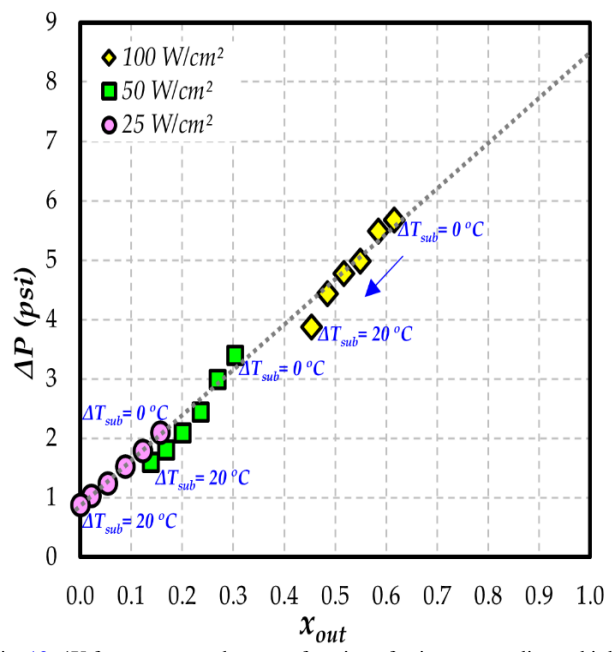


Fig. 12. 4X foam pressure drop as a function of exit vapor quality and inlet subcooling, ΔT_{sub} , at G of 150 kg/m²s and $T_{\text{sat, in}}$ of 30 °C

From the hydraulic performance standpoint, for fixed conditions, pressure drop significantly decreases with increasing subcooling, as illustrated in Fig. 11. Exit quality plot, illustrated in Fig. 12, shows that pressure drop curves derived from different subcooling and heat fluxes will collapse to a straight line. Data in Fig. 12, shows that pressure drop decreases with decrease in exit quality, as also previously reported in [6]. A curve fit for the pressure drop as a function of exit quality predicts the pressure drop at exit vapor quality of 100%, which is the highest. The decrease in pressure drop with increasing subcooling, thus the reduced exit vapor quality, is attributed to decrease in acceleration of the two-phase mixture as the vapor expands. From Fig. 12, the pressure drop is least for the zero exit quality due to single-phase flow dominance due to its lower friction factor compared to the two-phase flow counterpart.

III. CONCLUSIONS

Pumped two-phase flow experiments were conducted to investigate effects of foam compression ratio and refrigerant operating conditions, mainly including saturation temperature and subcooling on two-phase cooling performance using metallic foams. The following conclusions were reached, as detailed below:

- 1. Data show that thermal resistance in foam is a strong function of compression ratio (CR). At about 100 W/cm², compressing foam 4X and 2X foam reduces thermal resistance by 6.7 and 2.9 times, respectively, as compared to the uncompressed (1X) foam.
- In addition, from thermal performance standpoint, it is revealed that compressing the foam increases the optimal exit vapor quality at which maximum thermal performance

- occurs. Compared to 1X (uncompressed), data reveal that 4X and 2X foams increased the optimum exit vapor quality by 214% and 160%, respectively.
- 3. It is shown that foam two-phase flow CHF increases with compression ratio of copper foams. Data reveals that 4X and 2X foams enhanced CHF by about 2.4 and 1.9 times, respectively, compared to uncompressed (1X) foam
- 4. Related to CHF, results show that critical exit vapor quality for two-phase flow in foam increases with increase in compression ratio. In comparison to uncompressed foam, it is shown that 4X and 2X foams increase the critical exit quality by 2.23 and 1.17 times, respectively
- 5. As expected, pressure drop increases with increase in compression ratio due to decrease in pore hydraulic diameter and increase in foam surface area
- 6. Data reveal that the thermal resistance in 4X compressed foam decreases with increase in inlet saturation temperature, but the pressure drop has a weak dependence on the same
- Results show that increasing inlet subcooling significantly increases thermal resistance and decreases pressure drop in 4X compressed foam.
- 8. Compressed copper foams preliminary appear to be efficient alternatives to microchannels for pumped two-phase indirect cooling, though more investigations to compare the two technologies are needed.
- 9. The effects of metallic foam height on two-phase thermohydraulic performance should be studied.

ACKNOWLEDGMENT

This work is funded by the National Science Foundation Industry/University Collaborative Research Center (NSF I/UCRC) under Grant No. IIP-1738782. Any opinions, findings, and conclusions or recommendations expressed in this article are solely the responsibility of the authors and do not necessarily represent the official views of the NSF. ERG Aerospace Corporation is recognized for providing the copper foam test samples and for constructing the test section. Finally, Carol Caceres' contribution to this work is acknowledged.

REFERENCES

- [1] C. H. Hoang *et al.*, "A Review of Recent Developments in Pumped Two-Phase Cooling Technologies for Electronic Devices," *IEEE Transactions on Components, Packaging and Manufacturing Technology*, vol. 11, no. 10, pp. 1565–1582, Oct. 2021, doi: 10.1109/TCPMT.2021.3117572.
- [2] D. Kisitu and A. Ortega, "Thermal-Hydraulic Analytical Models of Split-Flow Microchannel Liquid-Cooled Cold Plates With Flow Impingement," presented at the ASME 2021 International Technical Conference and Exhibition on

- Packaging and Integration of Electronic and Photonic Microsystems, Nov. 2021. doi: 10.1115/IPACK2021-73283.
- [3] P. Rodgers, V. Eveloy, and M. G. Pecht, "Limits of air-cooling: status and challenges," in *Semiconductor Thermal Measurement and Management IEEE Twenty First Annual IEEE Symposium*, 2005., Mar. 2005, pp. 116–124. doi: 10.1109/STHERM.2005.1412167.
- [4] A. Ortega *et al.*, "Determination of the Thermal Performance Limits for Single Phase Liquid Cooling Using an Improved Effectiveness-NTU Cold Plate Model," presented at the ASME 2022 International Technical Conference and Exhibition on Packaging and Integration of Electronic and Photonic Microsystems, Dec. 2022. doi: 10.1115/IPACK2022-97421.
- [5] S. G. Kandlikar, "Heat Transfer Mechanisms During Flow Boiling in Microchannels," *Journal of Heat Transfer*, vol. 126, no. 1, pp. 8–16, Mar. 2004, doi: 10.1115/1.1643090.
- [6] D. Kisitu, C. Caceres, M. Zlatinov, D. Schaffarzick, and A. Ortega, "Experimental Investigation of R134a Flow Boiling in Copper Foam Evaporators for High Heat Flux Electronics Cooling," presented at the ASME 2022 International Technical Conference and Exhibition on Packaging and Integration of Electronic and Photonic Microsystems, Dec. 2022. doi: 10.1115/IPACK2022-97400.
- [7] D. W. Kim, A. Bar-Cohen, and B. Han, "Forced convection and flow boiling of a dielectric liquid in a foam-filled channel," in 2008 11th Intersociety Conference on Thermal and Thermomechanical Phenomena in Electronic Systems, May 2008, pp. 86–94. doi: 10.1109/ITHERM.2008.4544258.
- [8] I. Pranoto and K. C. Leong, "An experimental study of flow boiling heat transfer from porous foam structures in a channel," *Applied Thermal Engineering*, vol. 70, no. 1, pp. 100–114, Sep. 2014, doi: 10.1016/j.applthermaleng.2014.04.027.
- [9] B. Madani, L. Tadrist, and F. Topin, "Experimental analysis of upward flow boiling heat transfer in a channel provided with copper metallic foam," *Applied Thermal Engineering*, vol. 52, no. 2, pp. 336–344, Apr. 2013, doi: 10.1016/j.applthermaleng.2012.11.046.
- [10] K. E. Gungor and R. H. S. Winterton, "Simplified General Correlation For Saturated Flow Boiling And Comparisons Of Correlations With Data," *Chemical Engineering Research and Design*, vol. 65, no. 2, pp. 148–156, 1987.
- [11] S. Mancin, A. Diani, L. Doretti, and L. Rossetto, "R134a and R1234ze(E) liquid and flow boiling heat transfer in a high porosity copper foam," *International Journal of Heat and Mass Transfer*, vol. 74, pp. 77–87, Jul. 2014, doi: 10.1016/j.ijheatmasstransfer.2014.02.070.
- [12] A. Diani, S. Mancin, L. Doretti, and L. Rossetto, "Low-GWP refrigerants flow boiling heat transfer in a 5 PPI copper foam," *International Journal of Multiphase Flow*, vol. 76, pp. 111–121, Nov. 2015, doi: 10.1016/j.ijmultiphaseflow.2015.07.003.
- [13] B. Ozmat, B. Leyda, and B. Benson, "Thermal Applications of Open-Cell Metal Foams," *Materials and*

- Manufacturing Processes, vol. 19, no. 5, pp. 839–862, Oct. 2004, doi: 10.1081/AMP-200030568.
- [14] "PTM7000 Series | Honeywell." https://thermalmanagement.honeywell.com/us/en/products/the rmal-interface-materials/phase-change-materials/ptm7000-series (accessed Nov. 27, 2022).
- [15] "Copper Foam | Duocel® Open Cell Foam Foam," https://ergaerospace.com/. https://ergaerospace.com/copper-foam/ (accessed Apr. 25, 2022).
- [16] I. H. Bell, J. Wronski, S. Quoilin, and V. Lemort, "Pure and Pseudo-pure Fluid Thermophysical Property Evaluation and the Open-Source Thermophysical Property Library CoolProp," *Ind. Eng. Chem. Res.*, vol. 53, no. 6, pp. 2498–2508, Feb. 2014, doi: 10.1021/ie4033999.
- [17] R. J. Moffat, "Describing the uncertainties in experimental results," *Experimental Thermal and Fluid Science*, vol. 1, no. 1, pp. 3–17, Jan. 1988, doi: 10.1016/0894-1777(88)90043-X.
- [18] C. L. Ong and J. R. Thome, "Macro-to-microchannel transition in two-phase flow: Part 2 Flow boiling heat transfer and critical heat flux," *Experimental Thermal and Fluid Science*, vol. 35, no. 6, pp. 873–886, Sep. 2011, doi: 10.1016/j.expthermflusci.2010.12.003.